Published in final edited form as:
*Cell Tissue Res*. 2012 November ; 350(2): 261–275. doi:10.1007/s00441-012-1478-5.

# Translocator protein (*Tspo*) gene promoter-driven green fluorescent protein synthesis in transgenic mice: an *in vivo* model to study *Tspo* transcription

**Hui-Jie Wang**[1,2], **Jinjiang Fan**[1,2], and **Vassilios Papadopoulos**[1,2,3,4]

[1]The Research Institute of the McGill University Health Center, McGill University, Montréal, Québec H3A 1A4, Canada

[2]Department of Medicine, McGill University, Montréal, Québec H3A 1A4, Canada

[3]Department of Biochemistry, McGill University, Montréal, Québec H3A 1A4, Canada

[4]Department of Pharmacology & Therapeutics, McGill University, Montréal, Québec H3A 1A4, Canada

## Abstract

Translocator protein (TSPO), previously known as the peripheral-type benzodiazepine receptor, is a ubiquitous drug- and cholesterol-binding protein primarily found in the outer mitochondrial membrane as part of a mitochondrial cholesterol transport complex. TSPO is present at higher levels in steroid-synthesizing and rapidly proliferating tissues, and its biological role has been mainly linked to mitochondrial function, steroidogenesis, and cell proliferation/apoptosis. Aberrant TSPO levels have been linked to multiple diseases, including cancer, endocrine disorders, brain injury, neurodegeneration, ischemia-reperfusion injury, and inflammatory diseases. Investigation of the functions of this protein in vitro and in vivo have been mainly carried out using high-affinity drug ligands, such as isoquinoline carboxamides and benzodiazepines, and more recently, gene silencing methods. To establish a model to study the regulation of *Tspo* transcription in vivo, we generated a transgenic mouse model expressing green fluorescent protein (GFP) from *Aequorea coerulescens* under control of the *Tspo* promoter region (*Tspo*-AcGFP). The expression profiles of *Tspo*-AcGFP, endogenous TSPO, and *Tspo* mRNA were found to be well correlated. *Tspo*-AcGFP synthesis in the transgenic mice was seen in almost every tissue examined, and as with TSPO in wild-type mice, *Tspo*-AcGFP was highly expressed in steroidogenic cells of the endocrine and reproductive systems, epithelial cells of the digestive system, skeletal muscle, and other organs. In summary, this transgenic *Tspo*-AcGFP mouse model recapitulates endogenous *Tspo* expression patterns and could be a useful, tractable tool for monitoring the transcriptional regulation and function of *Tspo* in live animal experiments.

### Keywords

Translocator protein; AcGFP; promoter activity; immunohistochemistry; expression profile

Correspondence and reprint requests: Vassilios Papadopoulos. The Research Institute of the McGill University Health Centre, Montreal General Hospital, 1650 Cedar Avenue, Room C10-148, Montréal, Québec H3G 1A4, Canada. Tel: +1 514 934 1934, ext. 44580; Fax: +1 514 934 8439; vassilios.papadopoulos@mcgill.ca.

## Introduction

Translocator protein (TSPO), previously known as peripheral-type benzodiazepine receptor, was first described more than 30 years ago as the peripheral binding site for the benzodiazepine diazepam (Braestrup et al. 1977; Verma and Snyder 1989; Papadopoulos et al. 2006). TSPO function and distribution has been studied over the years using high-affinity drug ligands. Ro5-4864 (4′-chlorodiazepam) and PK 11195 (1-(2-chlorophenyl)-N-methyl-N-(1-methylpropyl)-3-isoquinolinecarboxamide) are the two most widely used TSPO drug ligands because of their high affinity, specificity, pharmacology, and ability to be modified. They have been used to explore TSPO distribution and function in various tissues and pathologies (Pellow and File 1984; Leong et al. 1996; Kuhlmann and Guilarte 1999; Chen et al. 2004; Veenman and Gavish 2006; Doorduin et al. 2008; Fujimura et al. 2008; Laitinen et al. 2009; Scarf and Kassiou 2011). These studies have included the use of radiolabeled compounds followed by autoradiography to map the “peripheral binding site,” which was found in almost every tissue examined (Anholt et al. 1985; De Souza et al. 1985). More recently, new structurally diverse TSPO drug ligands have been developed and used for functional and imaging studies (Rupprecht et al. 2010; Scarf and Kassiou, 2011).

With the development of TSPO-specific antisera, immunohistochemical assessment of TSPO presence demonstrated its selective localization in numerous healthy human tissues, including lung, stomach, small intestine, colon, thyroid, adrenal gland, pancreas, breast, prostate, and ovary, as well as in tumors that arise from these tissues (Hardwick et al. 1999; Han et al. 2003; Galiègue et al. 2004; Vlodavsky and Soustiel 2007; Ostuni et al. 2010). A similar pattern of TSPO localization was observed in the various tissues studied in various animal models, including mice, rats, and pigs (Papadopoulos 1993; Zisterer and Williams 1997; Papadopoulos et al. 2006; Veenman and Gavish 2006; Rupprecht et al. 2010). Elevated levels of TSPO, compared to controls, has been suggested as a potential drug target for cancer treatment (Decaudin 2004; Batarseh and Papadopoulos 2010) as well as a therapeutic target for neurological and psychiatric disorders (Rupprecht et al. 2010) and tissues undergoing ischemia-reperfusion injury (Zhang et al. 2006). Despite these advances in understanding TSPO function, current research on the regulation of tissue levels of TSPO lags due to the lack of an animal model that would allow us to study in vivo and in real time the dynamic changes in TSPO synthesis during disease progression and/or treatment. To monitor the temporal and spatial formation of TPSO in live animals, green fluorescent protein (GFP) synthesis driven by the *Tspo* promoter could be a useful tool to overcome this shortcoming.

Transgenic animals have been frequently used in a wide range of biological studies (Ristevski 2005). The use of GFP as a reporter gene has overcome some of the limits of using the traditional marker, *LacZ*, in transgenic animals, because GFP fluorescence allows for non-invasive imaging while providing excellent spatial and temporal resolution and the option to subsequently immunolabel the tissues with various antisera (Wang et al. 2011; Moore et al. 2011; Miller 2011). In 2007, we reported that *Tspo* promoter fragments extending 2.7 kb and 805 bp upstream of the transcription start site were able to direct enhanced GFP synthesis to the TSPO-rich Leydig cells of the testis, ovarian theca cells, and cells of the adrenal cortex (Giatzakis et al. 2007). We report herein the establishment of a new transgenic mouse line expressing *Tspo*-AcGFP (*Aequorea coerulescens* GFP), instead of the previously used enhanced GFP (Giatzakis et al. 2007). Although AcGFP1 shares 94% homology with enhanced GFP, it is translated more efficiently and is expressed more highly in mammalian cells (Haas et al. 1996). This is most likely because AcGFP is a monomer, whereas enhanced GFP undergoes dimerization (Haas et al. 1996). In this transgenic model, the *Tspo*-AcGFP synthesis pattern throughout the body is similar to that of endogenous

TSPO as assessed by immunohistochemistry and *Tspo* mRNA expression as assessed by microarray.

## Materials and methods

### 1. Generation of Tspo-AcGFP1 transgenic animals

Construction of *Tspo* 2.7-kb promoter-AcGFP1 plasmid was performed according to previously described methodology (Giatzakis et al. 2007). In brief, the 2.7-kb promoter fragment, which contains 32 bp of *Tspo* exon 1 from pGL3-2.7K, was subcloned into the pAcGFP1 plasmid vector (Clontech, Mountain View, CA, USA) immediately upstream of the open reading frame (ORF) for AcGFP1. The plasmid was linearized by cutting with *Afl*II and *Kpn*I and used to transfect the mouse embryonal carcinoma cell line F9 to measure levels of GFP synthesis. The DNA fragment was subsequently microinjected into pronuclei of fertilized mouse oocytes, and two-cell embryos were transferred to pseudo-pregnant foster female mice. The founders were identified by polymerase chain reaction (PCR) screening and bred for F1 phenotypic identification by fluorescence (Fig. 1A) using the ImageQuant LAS-4000 imaging system equipped with a blue-light-emitting diode (460nmEPI) and a band-pass filter for GFP (510DF10) (Fujifilm, Tokyo, Japan). Genotypic identification was performed by PCR using the following primers: a, ACAGACCTGTAGTCTGCTGGTC; b, AGGGTGGCTACTTTGACATGG; and c, CGACCACGCGTAAGAGCTCG; the flanking regions of the insertion were determined by reverse-PCR and genome walking as previously described (Ochman et al. 1988; Siebert et al. 1995) (Fig. 1B). All experimental protocols were approved by the McGill University Animal Care Committee.

### 2. Immunohistochemistry

Six weeks old adult male and female animals synthesizing AcGFP were euthanized by carbon dioxide inhalation, in accordance with the Animal Welfare Act and institutional guidelines. Tissues from positively genotyped mice were immediately collected, fixed in 10% neutral phosphate buffered formalin, and embedded in paraffin blocks. Paraffin blocks were sectioned (5 μm) for hematoxylin and eosin (H&E) staining and immunohistochemistry. Sections were also used to detect TSPO using an affinity-purified anti-peptide rabbit antiserum produced as previously described (Li et al. 2001). In brief, sections were deparaffinized, rehydrated, and treated with DAKO reagent (DAKO Corp, Glostrup, Denmark). The sections were incubated with the first antibody at 4 °C overnight and then with a biotin-conjugated secondary antibody (Invitrogen, Carlsbad, CA, USA). Immunoreactivity was detected using a streptavidin-horse radish peroxidase colorimetric reaction (Zymed, Carlsbad, CA, USA) and examined under bright-field microscopy with a BX40 Olympus microscope (Olympus America, Center Valley, PA, USA) coupled to a DP70 Olympus digital camera. Sections were counterstained with H&E, coated with Crystal Mount (Biomeda Corp, Foster City, CA, USA), and visualized by microscopy.

### 3. Confocal microscopy

Fresh tissue specimens were frozen in optimal cutting temperature (OCT) compound. Five-micrometer-thick sections were cut with a Leica CM1900 cryostat (Leica Microsystems, Wetzlar, Germany), placed in charged slides, counterstained with DAPI (Invitrogen, Cat # D3571), and mounted with antifade solution (Invitrogen, Cat # P-7481). Samples were analyzed and photographed using an Olympus Fluoview-FV1000 laser scanning confocal microscope (Olympus America) as previously described (Giatzakis et al. 2007). Background subtraction was carried out using the Olympus Fluoview version 3C software, setting the baseline fluorescence with the equivalent organs from a non-transgenic animal (data not shown).

### 4. Expression profile of Tspo mRNA

The mouse *Tspo* expression atlas was extracted from the tissue-specific pattern of mRNA expression study with NCBI-GEO #GSE1133 (http://www.ncbi.nlm.nih.gov/geo). A total of 61 mouse tissues were examined for *Tspo* (Su et al. 2004). The expression profile of the *Tspo2* gene from corresponding tissues was also extracted to compare with that of its paralogous gene, *Tspo*, which has been confirmed by *in situ* hybridization studies in whole body sections of tissues of all developmental stages, as previously described (Fan et al. 2009).

## Results and discussion

### Generation of a Tspo-AcGFP transgenic mouse strain

Four transgenic founder lines of *Tspo*-AcGFP mice were generated from the injection of 21 fertilized oocytes with linearized *Tspo*-AcGFP DNA fragments. The founder mice were backcrossed to wild-type mice. Each genotype was observed at the expected Mendelian frequency in the F1 generation. The transgenic mice were viable, fertile, appeared to be normal upon physical inspection, and expressed GFP throughout the body (Fig. 1A). The transgenic line with the highest levels of AcGFP was genotyped at the locus of chromosome 16, up-stream of the coordinate: mm9_dna range=chr16:80244117 (UCSC Genome Browser on Mouse July 2007 (NCBI37/mm9) Assembly; http://genome.ucsc.edu). Its identification sequence at the downstream of the locus is: CCCATCTTCCATAGAAACAATTTGCCTACTATGTCC. Fig. 1B and C). No annotated genes were found within 2.4 Mbp upstream and 7.0 Mbp downstream to the insertion site by blast analysis using the NCBI mouse build 37 genome database. This mouse line was used for further experiments and characterization.

### Tspo-AcGFP synthesis in the urogenital system

Although it seems that *Tspo*-AcGFP is synthesized at various levels in several cell types of the analyzed organs in transgenic mice, *Tspo*-AcGFP actually retained a cell- and tissue-specific synthesis pattern. The most studied function of TSPO is in cholesterol import into mitochondria, the rate-limiting step in hormone-stimulated steroidogenesis (Papadopoulos et al. 1991; Papadopoulos 1993; Gavish et al. 1999; Papadopoulos et al. 2006). Thus, we first evaluated TSPO and *Tspo*-AcGFP presence in the male reproductive tract (Fig. 2) and female urogenital system (Fig. 3). In the male reproductive system, the highest synthesis of AcGFP in testis was observed exclusively in interstitial Leydig cells (Fig. 2A-C). This observation is in agreement with previous findings obtained by autoradiography of [$^3$H]Ro5-4864 (De Souza et al. 1985), immunohistochemistry (Garnier et al. 1993), cell studies (Papadopoulos et al. 1990) and the *Tspo*-enhanced GFP studies (Giatzakis et al., 2007). Furthermore, it is consistent with the biological role of TSPO in steroid biosynthesis (Anholt et al. 1986; Papadopoulos et al. 1990; Papadopoulos et al. 1994; Giatzakis et al. 2007; Papadopoulos et al. 2007). In the head of the epididymis, AcGFP was observed in the Golgi area of the principal cells of the columnar epithelium (Fig. 2D-F). Previous reports using radioligand binding assays have shown that TSPO is expressed in epididymal adipose tissue (Campioli et al. 2010) and in the whole male genital tract (Katz et al. 1990; Gavish et al. 1999). This seems to be the first evidence for TSPO presence in the principal cells of epididymis. In addition, AcGFP synthesis was observed in most of the epithelium of the prostate and, to a lesser extent, in the seminal vesicles (Fig. 2 G-L). This observation is consistent with previous radioligand binding assays and immunohistochemical studies demonstrating the presence of TSPO in the prostate (Camins et al. 1992; Han et al. 2003; Fafalios et al. 2009).

In the female reproductive system, AcGFP was intensely seen in the theca cells and corpus luteum of ovary (Fig. 3A-F), but neither granulosa cells nor germinal vesicles displayed any fluorescence, in agreement with our previous studies using the 2.7-kb *Tspo* promoter region-driven enhanced GFP expression system (Giatzakis et al. 2007). The theca cells of the theca interna are responsible for the production of androstenedione and 17β estradiol, whereas the corpus luteum, as a temporary endocrine structure, is involved in the production of progesterone as well as estradiol (Smith et al. 1975; Fares et al. 1988; Gilling-Smith et al. 1994). In agreement with the TSPO immunohistochemical data, the presence of *Tspo*-AcGFP reflects the *Tspo* mRNA expression in these steroid-synthesizing tissues, implying its function in the transport of cholesterol into the mitochondria for steroid biosynthesis in concert with other partner proteins (Papadopoulos et al. 2007; Rone et al. 2009; Fan et al. 2010).

In the urinary system, we examined kidney and bladder sections and found that the epithelial cells of the distal and proximal tubules in the kidney (Fig. 3G-I) and the superficial epithelial cells in the urinary bladder (Fig. 3J-L) showed strong AcGFP synthesis as well as strong TSPO immunohistochemical staining. Previous reports have indicated that kidney is one of non-steroidogenic organs with high TSPO levels, even though some studies have suggested that the kidney might also be a steroid hormone-synthesizing organ (Gehlert et al. 1985; Gavish et al. 1999; Bribes et al. 2004; Pagotto et al. 2010), Components of the steroidogenic machinery, including the TSPO partner, the steroidogenic acute regulatory protein (STAR), are found in the distal tubules. Interestingly, estradiol has been reported to maintain TSPO density in kidney via post-transcriptional mechanisms (Pollack et al. 1997). TSPO in kidney has been proposed to play a role in renal protection and maintenance of kidney function (Katz et al. 1989; Holick 2007; Favreau et al. 2009), whereas in the urinary bladder, TSPO might play a role in altering contractility through modulation of calcium activity (Smyth et al. 1994).

### Tspo-AcGFP synthesis in the central nervous system

In the brain, TSPO levels are low overall and mainly found in glia and, at very low levels, in neurons (Veenman and Gavish 2006; Chen and Guilarte 2008; Papadopoulos and Lecanu 2009; Rupprecht et al. 2010). *Tspo* promoter-driven AcGFP synthesis was observed in the granule cell layer of the dentate gyrus and in the pyramidal cells of CA3 regions of the hippocampus and the Purkinje cells of the cerebellum, where TSPO staining was mostly observed in the nuclear/perinuclear area (Fig. 4). The immunohistochemical staining of TSPO is in agreement with previous radioligand (PK 11195) binding assays (Kuhlmann and Guilarte 2000). Although the regional localization of TSPO immunostaining and AcGFP fluorescence are similar, there are inconsistencies between the AcGFP and TSPO protein localization in the brain, as seen by the more widespread presence of TSPO compared to *Tspo* promoter-driven AcGFP. Nevertheless, perinuclear/nuclear localization of TSPO is not surprising and was previously reported in glial cells (Brown et al. 2000; Kuhlmann and Guilarte 2000). It is important to note that the intracellular localization of AcGFP and TSPO is determined by two distinct intracellular transport mechanisms due to the primary and secondary structure of the formed proteins and characterizing this is beyond the scope of this report (Otera et al. 2007; Rone et al. 2009b; Midzak et al. 2011).

Animal and human brain imaging following administration of radiolabeled TSPO drug ligands and positron emission tomography confirm that TSPO presence is low in the healthy brain (Veenman and Gavish, 2000; Chen and Guilarte, 2008; Papadopoulos and Lecanu, 2009; Rupprecht et al. 2010). In contrast, TSPO is upregulated in the brain at sites of injury and inflammation as well as following a number of neuropathological conditions in experimental animals and humans (Veenman and Gavish, 2000; Chen and Guilarte, 2008; Papadopoulos and Lecanu, 2009; Rupprecht et al., 2010). We believe that the *Tspo*-AcGFP

mouse offers an invaluable tool, to some extent, to decipher the cellular origin and regulation of the reported increase in TSPO levels in response to inflammation and injury.

### Tspo-AcGFP synthesis in the neuroendocrine and endocrine system

Of the neuroendocrine organs examined, *Tspo*-AcGFP was strongly expressed in the pars distalis of the pituitary gland (Fig. 5A-C) and the pineal gland (Fig. 5D-F). From the endocrine organs investigated, high levels of synthesis were seen in the epithelium of the thyroid gland (Fig. 5G-I) and the zona glomerulosa, fasciculata, and reticularis of the adrenal gland (Fig. 5J-L). The pars distalis (distal part) of the pituitary gland, where pituitary hormone production occurs, constitutes the majority of the anterior pituitary. TSPO in the anterior pituitary has been detected via autoradiographic localization of [$^{3}$H]Ro5-4864 (Grandison 1983; Souza et al. 1985). Other secretory and glandular tissues, such as the pineal gland, thyroid epithelium, and the adrenal glands, have been found to contain high levels of TSPO. PK 11195 radioligand binding studies have shown the presence of TSPO in the bovine pineal gland (Basile et al. 1986). *In situ* hybridization with $^{33}$P-labeled oligonucleotides demonstrated the presence of TSPO in the rat thyroid gland (Bürgi et al. 1999). Autoradiographic localization of radiolabeled Ro5-4864 (Souza et al. 1985), adrenal cell radioligand binding assays (Mukhin et al. 1989), immunohistochemistry (Oke et al. 1992), and our *Tspo* promoter-driven enhanced GFP mouse model (Giatzakis et al. 2007) have demonstrated the high level of TSPO in the adrenal gland.

### Tspo-AcGFP synthesis in the eye and the skin

*Tspo*-AcGFP was expressed in the epithelial cells of the ciliary body and cornea (Fig. 6A-F). Although *Tspo*-AcGFP fluorescence was not as strong as the TSPO immunohistochemical staining, the AcGFP synthesis patterns in the ciliary body and anterior corneal epithelia correlated well with TSPO levels. Previous PK 11195 radioligand binding assays in the eye reported the presence of TSPO in the corneal and ciliary epithelia (Zarbin and Anholt 1991). The remarkably high levels of TSPO in the ciliary epithelium raise the possibility that photodynamic therapy using hematoporphyrin, a TSPO drug ligand (Verma et al. 1987; Snyder et al. 1987; Taketani et al. 1995; Wendler et al. 2003), may be used in combination with subthermal cyclophotoirradiation to treat intraocular tumors and to induce vascular shutdown to treat macular degeneration (Liu and Ni 1983; Tse et al. 1984).

In the skin, *Tspo*-AcGFP was observed in hair follicles and the dermis reticular layer in patterns that correlate well with TSPO immunoreactivity (Fig. 6G-I). Human TSPO has previously been shown to be expressed selectively on the mitochondrial membranes of epidermal cells and hair follicles (Stoebner et al. 1999). The biological roles of highly expressed TSPO in the skin are likely related to the modulation of apoptosis in the epidermis as well as to natural skin protection against free radical damage generated by ultraviolet exposure (Stoebner et al. 1999). Indeed, as TSPO density is decreased in poorly differentiated and infiltrative skin carcinomas, such carcinomas may be effectively treated with photodynamic therapy (Morgan et al. 2004).

### Tspo-AcGFP synthesis in the digestive system

In addition to *Tspo*-AcGFP presence in the tongue (Fig. 7A-C), submandibular glands (Fig. 7D-F), esophagus (Fig. 7G-I), stomach (Fig. 7J-L), and liver (Fig. 7M-O), we report herein that *Tspo*-AcGFP is expressed in the simple columnar epithelium of the small intestine, which is lined up in a row at the base of the enterocytes with interspersed goblet cells, as well as in the columnar absorptive epithelium of the colon (Fig. 7P-U). It is obvious from the data presented that *Tspo*-AcGFP is distributed in almost all the epithelial cells of the digestive system, including the mucosal and submucosal layers of the gastric organs, indicating that TSPO is involved in the absorption and secretory functions of these organs.

*Tspo*-AcGFP synthesis in the tongue may be useful in monitoring the treatment of oral and esophageal cancers, since there is significantly enhanced TSPO levels in oral (Nagler et al. 2010) and esophageal (Sutter et al. 2002) cancers. However, the weak *Tspo*-AcGFP levels in the stratified squamous epithelium of the esophagus may indicate that the 2.7-kb *Tspo* promoter region may contain some transcription factor binding sites that have tissue-specific features or the genomic context of the insertion of the 2.7-kb *Tspo* promoter region has some tissue-specific features. A similar case may occur in the pars intermedia of pituitary gland, where no *Tspo*-AcGFP signal was detected (Fig. 5A-C).

Interestingly, the presence of *Tspo*-AcGFP is consistent with previous immunohistochemical analyses of TSPO in the mucous acinar cells and duct of rat submandibular glands, implying a role in modulating neurotransmitter-induced salivary secretion (Ostuni et al. 2008). Notably, TSPO is also expressed in hepatocytes, which supports previous reports of the presence of TSPO in the liver, demonstrated by radioligand binding assays (Woods et al. 1996) and northern blot analysis (Gazouli et al. 2002). In previous reports about the distribution and function of TSPO in rat small intestine, TSPO was found in enterocyte mitochondria with distinct pharmacological characteristics in different regions of the intestine, implying specific structural organization of mitochondrial protein complexes destined to convey either chloride secretion or absorption in the duodenum and ileum, respectively (Ostuni et al. 2004; Ostuni et al. 2007; Ostuni et al. 2009).

### Tspo-AcGFP synthesis in the cardiovascular system

Radioligand binding studies demonstrated that heart membranes contain high levels of TSPO, and TSPO ligand binding in the ventricles was higher than in the atria (Veenman and Gavish 2006). These results were confirmed by autoradiography of radiolabeled Ro5-4864 (Gehlert et al. 1985). In the present study, the main cell types in the heart where *Tspo*-AcGFP and TSPO were present were found in the myocardium, the muscular tissue of the heart (Fig. 8). A similar expression pattern has been reported in rat heart (Davies and Huston 1981; Holck and Osterrieder 1985; Yamamura et al. 1985; French and Matlib 1988). Cardiomyocytes have been extensively used to study the role of TSPO and TSPO drug ligands on ischemia-reperfusion injury via inhibition of mitochondrial membrane permeabilization (Veenman and Gavish 2006; Obame et al. 2007).

### Tspo-AcGFP synthesis in the respiratory system

The main cell type expressing *Tspo*-AcGFP and TSPO in the respiratory system were the ciliated columnar epithelial cells (Fig. 9). Previous work studying the distribution of the binding of the TSPO ligand [$^3$H]Ro5-4864 by autoradiography in human and guinea pig lungs indicated that epithelia had a higher grain density (Mak and Barnes 1990). The presence of TSPO in alveolar type II cells may be related to the increased secretion of surfactant through its effects on increased $Ca^{2+}$ efflux (Das and Mukherjee 1999). Moreover, TSPO drug ligands were shown to modulate the relaxation response of the guinea pig isolated trachea to adenosine (Advenier et al. 1990).

### Tspo-AcGFP synthesis in skeletal muscle and the hematopoietic system

Strong presence of *Tspo*-AcGFP was observed in the skeletal muscle (Fig. 10A-C), whereas only sparse synthesis of *Tspo*-AcGFP was found in bone marrow, with the exception of the megakaryocytes (Fig. 10D-F). The role of TSPO in the muscle may be related to muscle contraction (Chiou and Chang 1994). High levels of TSPO were found in rat bone marrow, the site of blood cell formation (Anholt et al. 1985). TSPO in bone marrow has been shown to participate in the protection of hematopoietic cells against oxygen radical damage (Carayon et al. 1996). Interestingly, *Tspo2*, a paralogous gene of *Tspo*, was found to be

specifically expressed in the mouse hematopoietic system, such as the bone marrow and spleen (Fan et al. 2009). The subcellular compartment-specific distribution of TSPO2 suggests that the two proteins from the same gene family possess distinct biological functions.

## Correlation between mouse Tspo expression profile from DNA microarray and Tspo-AcGFP in transgenic mice

From the expression profile of *Tspo* mRNA in 61 tissues/cell lines from a DNA microarray (GSE1133), it can be concluded that the expression patterns of *Tspo*-AcGFP and endogenous TSPO demonstrated here correlate well with the intensity of the microarray Affymetrix readings (Fig. 11). All of the tissues we examined using *Tspo*-AcGFP have been marked in red bars as shown in Fig. 11. The tissues/cells with the highest expression levels of *Tspo* mRNA detected in the DNA microarray are C2C12 cells, which are mouse myoblast cells and have been used to study the differentiation of myoblasts and osteoblasts (Yaffe and Saxel 1977). The high expression of *Tspo*-AcGFP in skeletal muscle is strikingly significant as shown in Fig. 10A-C. The tissues/cells with the second highest levels of *Tspo* mRNA are adipose tissue and the adrenal gland. *Tspo* expression has been reported during mouse and human adipocyte differentiation (Wade et al. 2005; Campioli et al. 2011), and TSPO drug ligands have been shown to play a role in adipose differentiation and proliferation of human mesenchymal stem cells (Lee et al. 2004). The high expression of *Tspo* mRNA and TSPO protein in the steroidogenic adrenal gland has been well established (Oke et al. 1992; Giatzakis and Papadopoulos 2004; Giatzakis et al. 2007). In some tissues composed of diverse cell populations, the tissue array does not allow for the specific analysis of the TSPO-rich component(s), as is the case with testis Leydig cells. As a general impression, *Tspo* mRNA seems to be expressed with variability in almost every tissue, but both oocytes and fertilized eggs have noticeably lower signals than the other tissues, which indicate lower expression or absence of *Tspo*. Nevertheless, we observed both *Tspo* mRNA and *Tspo*-AcGFP in mouse ovaries, and the selective localization of TSPO in the theca cells of this organ supports a role of TSPO in steroid biosynthesis (Giatzakis et al. 2007).

To validate this comparison, we also extracted the expression profile of *Tspo2*, which is a paralogous gene of *Tspo* with a hematopoietic tissue-specific expression pattern (Fan et al. 2009). The results obtained demonstrate that the expression profile of *Tspo2* strongly correlates with our previous report obtained by *in situ* hybridization (Fan et al. 2009). These data not only confirm the quality of the microarray data used for evaluation of *Tspo* gene tissue distribution but also raises attention to studies examining TSPO distribution in hematopoetic tissues where both TSPO and TSPO2 may be recognized by the antisera used.

Taken together, these results demonstrate that the DNA microarray data and the immunohistochemistry results reflecting tissue-specific endogenous *Tspo* mRNA and TSPO protein expression correlate well with the synthesis of *Tspo*-AcGFP in the transgenic mice. It is important to note that the presence of mouse TSPO and *Tspo*-AcGFT show an expression pattern similar to that reported for human TSPO in the prostate, ovary, breast, thyroid, adrenal gland, lung, stomach, small intestine, colon, and pancreas (Bribes et al. 2004). The high level of expression of TSPO and *Tspo*-AcGFT in steroidogenic cells confirms previous work demonstrating the important role of this protein in steroidogenesis (Papadopoulos 1993; Papadopoulos et al., 2006). The widespread presence of *Tspo*-AcGFP in epithelial cells suggests an important function of TSPO in non-steroidogenic cells as well. Epithelial cells respond to stress and injury, such as ischemia, chemicals, and infection by rapidly proliferating and restoring the integrity of the epithelium (Lacy 1988; Mammen and Matthews 2003). Unveiling the mechanism underlying the induction of proliferation and epithelial tissue restoration may help us understand the role played by TSPO in various tumors (Batarseh et al., 2010).

In conclusion, the *Tspo*-AcGFP transgenic model mimics the native expression of *Tspo in vivo*, thus providing a tractable tool for monitoring the regulation of *Tspo* expression in response to various stimuli or pathological conditions in live animal experiments to improve our understanding of the various tissue-specific biological roles of TSPO.

## Acknowledgments

The authors would like to acknowledge Dr. Louis Dettin for his assistance and Dr. Laurent Lecanu for help with the brain data analysis. This work was supported by grants from the National Institutes of Health (R01 ES07747) and the Canadian Institutes of Health Research (MOP 102647) to V.P. V.P. was also supported by a Canada Research Chair in Biochemical Pharmacology. The Research Institute of the MUHC was supported by a center grant from Le Fonds de la recherche du Québec - Santé.

## References

Advenier C, Devillier P, Blanc M, Gnassounou JP. Peripheral type benzodiazepine receptors and response to adenosine on the guinea-pig isolated trachea. Pulm Pharmacol. 1990; 3:137–144. [PubMed: 1966906]

Anholt RR, De Souza EB, Oster-Granite ML, Snyder SH. Peripheral-type benzodiazepine receptors: autoradiographic localization in whole-body sections of neonatal rats. J Pharmacol Exp Ther. 1985; 233:517–526. [PubMed: 2987488]

Anholt RR, Pedersen PL, De Souza EB, Snyder SH. The peripheral-type benzodiazepine receptor. Localization to the mitochondrial outer membrane. J Biol Chem. 1986; 261:576–583. [PubMed: 3001071]

Basile AS, Klein DC, Skolnick P. Characterization of benzodiazepine receptors in the bovine pineal gland: evidence for the presence of an atypical binding site. Mol Brain Res. 1986; 1:127–135.

Batarseh A, Papadopoulos V. Regulation of translocator protein 18 kDa (TSPO) expression in health and disease states. Mol Cell Endocrinol. 2010; 327:1–12. [PubMed: 20600583]

Braestrup C, Albrechtsen R, Squires RF. High densities of benzodiazepine receptors in human cortical areas. Nature. 1977; 269:702–704. [PubMed: 22814]

Bribes E, Carriere D, Goubet C, Galiegue S, Casellas P, Simony-Lafontaine J. Immunohistochemical assessment of the peripheral benzodiazepine receptor in human tissues. J Histochem Cytochem. 2004; 52:19–28. [PubMed: 14688214]

Brown RC, Degenhardt B, Kotoula M, Papadopoulous V. Location-dependent role of the human glioma cell peripheral-type benzodiazepine receptor in proliferation and steroid biosynthesis. Cancer Lett. 2000; 156:125–132. [PubMed: 10880761]

Bürgi B, Lichtensteiger W, Lauber ME, Schlumpf M. Ontogeny of diazepam binding inhibitor/acyl-CoA binding protein mRNA and peripheral benzodiazepine receptor mRNA expression in the rat. J Neuroendocrinol. 1999; 11:85–100. [PubMed: 10048463]

Camins A, Sureda FX, Camarasa J, Escubedo E. Specific binding sites for [$^{3}$H] Ro 5-4864 in rat prostate and seminal vesicle. Gen Pharmacol. 1992; 23:381–384. [PubMed: 1324864]

Campioli E, Batarseh A, Li J, Papadopoulos V. The endocrine disruptor mono-(2-ethylhexyl) phthalate affects the differentiation of human liposarcoma cells (SW 872). PLoS One. 2011; 6:e28750. [PubMed: 22205965]

Campioli E, Carnevale G, Avallone R, Guerra D, Baraldi M. Morphological and receptorial changes in the epididymal adipose tissue of rats subjected to a stressful stimulus. Obesity. 2010; 19:703–708. [PubMed: 20948513]

Carayon P, Portier M, Dussossoy D, Bord A, Petitpretre G, Canat X, Le FG, Casellas P. Involvement of peripheral benzodiazepine receptors in the protection of hematopoietic cells against oxygen radical damage. Blood. 1996; 87:3170–3178. [PubMed: 8605331]

Chen MK, Baidoo K, Verina T, Guilarte TR. Peripheral benzodiazepine receptor imaging in CNS demyelination: functional implications of anatomical and cellular localization. Brain. 2004; 127:1379–1392. [PubMed: 15069023]

Chen MK, Guilarte TR. Translocator protein 18 kDa (TSPO): molecular sensor of brain injury and repair. Pharmacol Ther. 2008; 118:1–17. [PubMed: 18374421]

Chiou LC, Chang CC. Pharmacological relevance of peripheral type benzodiazepine receptors on motor nerve and skeletal muscle. Br J Pharmacol. 1994; 112:257–261. [PubMed: 8032647]

Das SK, Mukherjee S. Role of peripheral benzodiazepine receptors on secretion of surfactant in guinea pig alveolar type II cells. Biosci Rep. 1999; 19:461–471. [PubMed: 10763813]

Davies LP, Huston V. Peripheral benzodiazepine binding sites in heart and their interaction with dipyridamole. Eur J Pharmacol. 1981; 73:209–211. [PubMed: 6273185]

De Souza EB, Anholt RR, Murphy KM, Snyder SH, Kuhar MJ. Peripheral-type benzodiazepine receptors in endocrine organs: autoradiographic localization in rat pituitary, adrenal, and testis. Endocrinology. 1985; 116:567–573. [PubMed: 2981667]

Decaudin D. Peripheral benzodiazepine receptor and its clinical targeting. Anticancer Drugs. 2004; 15:737. [PubMed: 15494634]

Doorduin J, De Vries EFJ, Dierckx RA, Klein HC. PET imaging of the peripheral benzodiazepine receptor: monitoring disease progression and therapy response in neurodegenerative disorders. Curr Pharm Des. 2008; 14:3297–3315. [PubMed: 19075709]

Fafalios A, Akhavan A, Parwani AV, Bies RR, McHugh KJ, Pflug BR. Translocator protein blockade reduces prostate tumor growth. Clin Cancer Res. 2009; 15:6177–6184. [PubMed: 19789311]

Fan J, Liu J, Culty M, Papadopoulos V. Acyl-coenzyme A binding domain containing 3 (ACBD3; PAP7; GCP60): an emerging signaling molecule. Prog Lipid Res. 2010; 49:218–234. [PubMed: 20043945]

Fan J, Rone MB, Papadopoulos V. Translocator protein 2 is involved in cholesterol redistribution during erythropoiesis. J Biol Chem. 2009; 284:30484–30497. [PubMed: 19729679]

Fares F, Bar-Ami S, Brandes JM, Gavish M. Changes in the density of peripheral benzodiazepine binding sites in genital organs of the female rat during the oestrous cycle. J Reprod Fertil. 1988; 83:619–625. [PubMed: 2842497]

Favreau F, Rossard L, Zhang K, Desurmont T, Manguy E, Belliard A, Fabre S, Liu J, Han Z, Thuillier R, Papadopoulos V, Hauet T. Expression and modulation of translocator protein and its partners by hypoxia reoxygenation or ischemia and reperfusion in porcine renal models. Am J Physiol Renal Physiol. 2009; 297:F177–F190. [PubMed: 19386723]

French JF, Matlib MA. Identification of a high-affinity peripheral-type benzodiazepine binding site in rat aortic smooth muscle membranes. J Pharmacol Exp Ther. 1988; 247:23–28. [PubMed: 2845053]

Fujimura Y, Hwang PM, Trout H III, Kozloff L, Imaizumi M, Innis RB, Fujita M. Increased peripheral benzodiazepine receptors in arterial plaque of patients with atherosclerosis: An autoradiographic study with [$^{3}$H] PK 11195. Atherosclerosis. 2008; 201:108–111. [PubMed: 18433754]

Galiègue S, Casellas P, Kramar A, Tinel N, Simony-Lafontaine J. Immunohistochemical assessment of the peripheral benzodiazepine receptor in breast cancer and its relationship with survival. Clin Cancer Res. 2004; 10:2058–2064. [PubMed: 15041726]

Garnier M, Boujrad N, Oke BO, Brown AS, Riond J, Ferrara P, Shoyab M, Suarez-Quian CA, Papadopoulos V. Diazepam binding inhibitor is a paracrine/autocrine regulator of Leydig cell proliferation and steroidogenesis: action via peripheral-type benzodiazepine receptor and independent mechanisms. Endocrinology. 1993; 132:444–458. [PubMed: 8380386]

Gavish M, Bachman I, Shoukrun R, Katz Y, Veenman L, Weisinger G, Weizman A. Enigma of the peripheral benzodiazepine receptor. Pharmacol Rev. 1999; 51:629–650. [PubMed: 10581326]

Gazouli M, Yao ZX, Boujrad N, Corton JC, Culty M, Papadopoulos V. Effect of peroxisome proliferators on Leydig cell peripheral-type benzodiazepine receptor gene expression, hormone-stimulated cholesterol transport, and steroidogenesis: role of the peroxisome proliferator-activator receptor alpha. Endocrinology. 2002; 143:2571. [PubMed: 12072389]

Gehlert DR, Yamamura HI, Wamsley JK. Autoradiographic localization of “peripheral-type” benzodiazepine binding sites in the rat brain, heart and kidney. Naunyn Schmiedebergs Arch Pharmacol. 1985; 328:454–460. [PubMed: 2986017]

Giatzakis C, Batarseh A, Dettin L, Papadopoulos V. The role of Ets transcription factors in the basal transcription of the translocator protein (18 kDa). Biochemistry. 2007; 46:4763–4774. [PubMed: 17402746]

Giatzakis C, Papadopoulos V. Differential utilization of the promoter of peripheral-type benzodiazepine receptor by steroidogenic versus nonsteroidogenic cell lines and the role of Sp1 and Sp3 in the regulation of basal activity. Endocrinology. 2004; 145:1113–1123. [PubMed: 14630713]

Gilling-Smith C, Willis DS, Beard RW, Franks S. Hypersecretion of androstenedione by isolated thecal cells from polycystic ovaries. J Clin Endocrinol Metab. 1994; 79:1158–1165. [PubMed: 7962289]

Grandison L. Actions of benzodiazepines on the neuroendocrine system. Neuropharmacology. 1983; 22:1505–1510. [PubMed: 6322044]

Haas J, Park EC, Seed B. Codon usage limitation in the expression of HIV-1 envelope glycoprotein. Curr Biol. 1996; 6:315–324. [PubMed: 8805248]

Han Z, Slack RS, Li W, Papadopoulos V. Expression of peripheral benzodiazepine receptor (PBR) in human tumors: relationship to breast, colorectal, and prostate tumor progression. J Recept Signal Transduct Res. 2003; 23:225–238. [PubMed: 14626449]

Hardwick M, Fertikh D, Culty M, Li H, Vidic B, Papadopoulos V. Peripheral-type benzodiazepine receptor (PBR) in human breast cancer: correlation of breast cancer cell aggressive phenotype with PBR expression, nuclear localization, and PBR-mediated cell proliferation and nuclear transport of cholesterol. Cancer Res. 1999; 59:831–842. [PubMed: 10029072]

Holck M, Osterrieder W. The peripheral, high affinity benzodiazepine binding site is not coupled to the cardiac $Ca^{2+}$ channel. Eur J Pharmacol. 1985; 118:293–301. [PubMed: 2417868]

Holick MF. Vitamin D deficiency. N Engl J Med. 2007; 357:266–281. [PubMed: 17634462]

Katz Y, Amiri Z, Weizman A, Gavish M. Identification and distribution of peripheral benzodiazepine binding sites in male rat genital tract. Biochem Pharmacol. 1990; 40:817–820. [PubMed: 2167096]

Katz Y, Moskovitz B, Levin DR, Gavish M. Absence of peripheral-type benzodiazepine binding sites in renal carcinoma: a potential biochemical marker. Br J Urol. 1989; 63:124–127. [PubMed: 2539222]

Kuhlmann AC, Guilarte TR. Regional and temporal expression of the peripheral benzodiazepine receptor in MPTP neurotoxicity. Toxicol Sci. 1999; 48:107–116. [PubMed: 10330690]

Kuhlmann AC, Guilarte TR. Cellular and subcellular localization of peripheral benzodiazepine receptors after trimethyltin neurotoxicity. J Neurochem. 2000; 74:1694–1704. [PubMed: 10737628]

Lacy ER. Epithelial restitution in the gastrointestinal tract. J Clin Gastroenterol. 1988; 10(1):S72–S77. [PubMed: 3053884]

Laitinen I, Marjamäki P, Någren K, Laine VJO, Wilson I, Leppänen P, Ylä-Herttuala S, Roivainen A, Knuuti J. Uptake of inflammatory cell marker [$^{11}$C] PK11195 into mouse atherosclerotic plaques. Eur J Nucl Med Mol Imaging. 2009; 36:73–80. [PubMed: 18712383]

Lee DH, Kang SK, Lee RH, Ryu JM, Park HY, Choi HS, Bae YC, Suh KT, Kim YK, Jung JS. Effects of peripheral benzodiazepine receptor ligands on proliferation and differentiation of human mesenchymal stem cells. J Cell Physiol. 2004; 198:91–99. [PubMed: 14584048]

Leong DK, Oliva L, Butterworth RF. Quantitative autoradiography using selective radioligands for central and peripheral-yype benzodiazepine receptors in experimental wernicke's encephalopathy: implications for positron emission tomography imaging. Alcohol Clin Exp Res. 1996; 20:601–605. [PubMed: 8727262]

Li H, Yao Z, Degenhardt B, Teper G, Papadopoulos V. Cholesterol binding at the cholesterol recognition/ interaction amino acid consensus (CRAC) of the peripheral-type benzodiazepine receptor and inhibition of steroidogenesis by an HIV TAT-CRAC peptide. Proc Natl Acad Sci U S A. 2001; 98:1267–1272. [PubMed: 11158628]

Liu LHS, Ni C. Hematoporphyrin phototherapy for experimental intraocular malignant melanoma. Arch Ophthalmol. 1983; 101:901–903. [PubMed: 6860202]

Mak JC, Barnes PJ. Peripheral type benzodiazepine receptors in human and guinea pig lung: characterization and autoradiographic mapping. J Pharmacol Exp Ther. 1990; 252:880. [PubMed: 2156066]

Mammen JM, Matthews JB. Mucosal repair in the gastrointestinal tract. Crit Care Med. 2003; 31:S532–S537. [PubMed: 12907883]

Midzak A, Rone M, Aghazadeh Y, Culty M, Papadopoulos V. Mitochondrial protein import and the genesis of steroidogenic mitochondria. Mol Cell Endocrinol. 2011; 336:70–79. [PubMed: 21147195]

Miller RL. Transgenic mice: beyond the knockout. Am J Physiol Renal Physiol. 2011; 300:F291–F300. [PubMed: 21068085]

Moore AM, Borschel GH, Santosa KA, Flagg ER, Tong AY, Kasukurthi R, Newton P, Yan Y, Hunter DA, Johnson PJ. A transgenic rat expressing green fluorescent protein (GFP) in peripheral nerves provides a new hindlimb model for the study of nerve injury and regeneration. J Neurosci Methods. 2011; 204:19–27. [PubMed: 22027490]

Morgan J, Oseroff AR, Cheney RT. Expression of the peripheral benzodiazepine receptor is decreased in skin cancers in comparison with normal skin. Br J Dermatol. 2004; 151:846–856. [PubMed: 15491426]

Mukhin AG, Papadopoulos V, Costa E, Krueger KE. Mitochondrial benzodiazepine receptors regulate steroid biosynthesis. Proc Natl Acad Sci U S A. 1989; 86:9813. [PubMed: 2574864]

Nagler R, Ben-Izhak O, Savulescu D, Krayzler E, Akrish S, Leschiner S, Otradnov I, Zeno S, Veenman L, Gavish M. Oral cancer, cigarette smoke and mitochondrial 18 kDa translocator protein (TSPO)--In vitro, in vivo, salivary analysis. Biochim Biophys Acta. 2010; 1802:454–461. [PubMed: 20085808]

Obame FN, Zini R, Souktani R, Berdeaux A, Morin D. Peripheral benzodiazepine receptor-induced myocardial protection is mediated by inhibition of mitochondrial membrane permeabilization. J Pharmacol Exp Ther. 2007; 323:336–345. [PubMed: 17640950]

Ochman H, Gerber AS, Hartl DL. Genetic applications of an inverse polymerase chain reaction. Genetics. 1988; 120:621–623. [PubMed: 2852134]

Oke BO, Suarez-Quian CA, Riond J, Ferrara P, Papadopoulos V. Cell surface localization of the peripheral-type benzodiazepine receptor (PBR) in adrenal cortex. Mol Cell Endocrinol. 1992; 87:R1–R6. [PubMed: 1332905]

Ostuni MA, Ducroc R, Peranzi G, Tonon MC, Papadopoulos V, Lacapere JJ. Translocator protein (18 kDa) ligand PK 11195 induces transient mitochondrial $Ca^{2+}$ release leading to transepithelial Cl- secretion in HT-29 human colon cancer cells. Biol Cell. 2007; 99:639–647. [PubMed: 17561806]

Ostuni MA, Issop L, Péranzi G, Walker F, Fasseu M, Elbim C, Papadopoulos V, Lacapere JJ. Overexpression of translocator protein in inflammatory bowel disease: Potential diagnostic and treatment value. Inflamm Bowel Dis. 2010; 16:1476–1487. [PubMed: 20222126]

Ostuni MA, Marazova K, Peranzi G, Vidic B, Papadopoulos V, Ducroc R, Lacapere JJ. Functional characterization and expression of PBR in rat gastric mucosa: stimulation of chloride secretion by PBR ligands. Am J Physiol Gastrointest Liver Physiol. 2004; 286:G1069–G1080. [PubMed: 14726306]

Ostuni MA, Peranzi G, Ducroc RA, Fasseu M, Vidic B, Dumont J, Papadopoulos V, Lacapere JJ. Distribution, pharmacological characterization and function of the 18 kDa translocator protein in rat small intestine. Biol Cell. 2009; 101:573–586. [PubMed: 19392661]

Ostuni MA, Tumilasci OR, Peranzi G, Cardoso EM, Contreras LN, Arregger AL, Papadopoulos V, Lacapere JJ. Effect of translocator protein (18 kDa)-ligand binding on neurotransmitter-induced salivary secretion in rat submandibular glands. Biol Cell. 2008; 100:427–439. [PubMed: 18269350]

Otera H, Taira Y, Horie C, Suzuki Y, Suzuki H, Setoguchi K, Kato H, Oka T, Mihara K. A novel insertion pathway of mitochondrial outer membrane proteins with multiple transmembrane segments. The Journal of cell biology. 2007; 179:1355–1363. [PubMed: 18158327]

Pagotto MA, Roldan ML, Pagotto RM, Lugano MC, Pisani GB, Rogic G, Molinas SM, Trumper L, Pignataro OP, Monasterolo LA. Localization and functional activity of Cytochrome P450 side chain cleavage enzyme (CYP11A1) in the adult rat kidney. Mol Cell Endocrinol. 2010; 332:253–260. [PubMed: 21075169]

Papadopoulos V. Peripheral-type benzodiazepine/diazepam binding inhibitor receptor: biological role in steroidogenic cell function. Endocr Rev. 1993; 14:222–240. [PubMed: 8391980]

Papadopoulos V, Baraldi M, Guilarte TR, Knudsen TB, Lacapere JJ, Lindemann P, Norenberg MD, Nutt D, Weizman A, Zhang MR, Gavish M. Translocator protein (18kDa): new nomenclature for

the peripheral-type benzodiazepine receptor based on its structure and molecular function. Trends Pharmacol Sci. 2006; 27:402–409. [PubMed: 16822554]

Papadopoulos V, Boujrad N, Ikonomovic MD, Ferrara P, Vidic B. Topography of the Leydig cell mitochondrial peripheral-type benzodiazepine receptor. Mol Cell Endocrinol. 1994; 104:R5–R9. [PubMed: 7821699]

Papadopoulos V, Lecanu L. Translocator protein (18 kDa) TSPO: an emerging therapeutic target in neurotrauma. Exp Neurol. 2009; 219:53–57. [PubMed: 19409385]

Papadopoulos V, Liu J, Culty M. Is there a mitochondrial signaling complex facilitating cholesterol import? Mol Cell Endocrinol. 2007:265–266. 59–64.

Papadopoulos V, Mukhin AG, Costa E, Krueger KE. The peripheral-type benzodiazepine receptor is functionally linked to Leydig cell steroidogenesis. J Biol Chem. 1990; 265:3772–3779. [PubMed: 2154488]

Papadopoulos V, Nowzari FB, Krueger KE. Hormone-stimulated steroidogenesis is coupled to mitochondrial benzodiazepine receptors. Tropic hormone action on steroid biosynthesis is inhibited by flunitrazepam J Biol Chem. 1991; 266:3682–3687.

Pellow S, File SE. Behavioural actions of Ro 5-4864: a peripheral-type benzodiazepine? Life Sci. 1984; 35:229–240. [PubMed: 6087055]

Pollack SE, Furth EE, Kallen CB, Arakane F, Kiriakidou M, Kozarsky KF, Strauss JF III. Localization of the steroidogenic acute regulatory protein in human tissues. J Clin Endocrinol Metab. 1997; 82:4243–4251. [PubMed: 9398748]

Ristevski S. Making better transgenic models. Mol Biotechnol. 2005; 29:153–163. [PubMed: 15699570]

Rone MB, Fan J, Papadopoulos V. Cholesterol transport in steroid biosynthesis: role of protein-protein interactions and implications in disease states. Biochim Biophys Acta. 2009a; 1791:646–658. [PubMed: 19286473]

Rone MB, Liu J, Blonder J, Ye X, Veenstra TD, Young JC, Papadopoulos V. Targeting and insertion of the cholesterol-binding translocator protein into the outer mitochondrial membrane. Biochemistry. 2009b; 48:6909–6920. [PubMed: 19552401]

Rupprecht R, Papadopoulos V, Rammes G, Baghai TC, Fan J, Akula N, Groyer G, Adams D, Schumacher M. Translocator protein (18 kDa)(TSPO) as a therapeutic target for neurological and psychiatric disorders. Nat Rev Drug Discov. 2010; 9:971–988. [PubMed: 21119734]

Scarf AM, Kassiou M. The translocator protein. J Nucl Med. 2011; 52:677–680. [PubMed: 21498529]

Siebert PD, Chenchik A, Kellogg DE, Lukyanov KA, Lukyanov SA. An improved PCR method for walking in uncloned genomic DNA. Nucleic Acids Res. 1995; 23:1087–1088. [PubMed: 7731798]

Smith MS, Freeman ME, Neill JD. The control of progesterone secretion during the estrous cycle and early pseudopregnancy in the rat: prolactin, gonadotropin and steroid levels associated with rescue of the corpus luteum of pseudopregnancy. Endocrinology. 1975; 96:219. [PubMed: 1167352]

Smyth RJ, Uhlman EJ, Ruggieri MR. Identification and characterization of a high-affinity peripheral-type benzodiazepine receptor in rabbit urinary bladder. J Urol. 1994; 151:1102–1106. [PubMed: 8126801]

Snyder SH, Verma A, Trifiletti RR. The peripheral-type benzodiazepine receptor: a protein of mitochondrial outer membranes utilizing porphyrins as endogenous ligands. FASEB J. 1987; 1:282–288. [PubMed: 2820823]

Souza EB, Anholt RRH, Murphy KMM, Snyder SH, Kuhar MJ. Peripheral-type benzodiazepine receptors in endocrine organs: autoradiographic localization in rat pituitary, adrenal, and testis. Endocrinology. 1985; 116:567–573. [PubMed: 2981667]

Stoebner PE, Carayon P, Penarier G, Frechin N, Barneon G, Casellas P, Cano JP, Meynadier J, Meunier L. The expression of peripheral benzodiazepine receptors in human skin: the relationship with epidermal cell differentiation. Br J Dermatol. 1999; 140:1010–1016. [PubMed: 10354064]

Su AI, Wiltshire T, Batalov S, Lapp H, Ching KA, Block D, Zhang J, Soden R, Hayakawa M, Kreiman G. A gene atlas of the mouse and human protein-encoding transcriptomes. Proc Natl Acad Sci U S A. 2004; 101:6062–6067. [PubMed: 15075390]

Sutter AP, Maaser K, Höpfner M, Barthel B, Grabowski P, Faiss S, Carayon P, Zeitz M, Scherübl H. Specific ligands of the peripheral benzodiazepine receptor induce apoptosis and cell cycle arrest in human esophageal cancer cells. Int J Cancer. 2002; 102:318–327. [PubMed: 12402299]

Taketani S, Kohno H, Furukawa T, Tokunaga R. Involvement of peripheral-type benzodiazepine receptors in the intracellular transport of heme and porphyrins. J Biochem. 1995; 117:875–880. [PubMed: 7592553]

Tse DT, Dutton JJ, Weingeist TA, Hermsen VM, Kersten RC. Hematoporphyrin photoradiation therapy for intraocular and orbital malignant melanoma. Arch Ophthalmol. 1984; 102:833–838. [PubMed: 6233958]

Veenman L, Gavish M. Peripheral-type benzodiazepine receptors: Their implication in brain disease. Drug development research. 2000; 50:355–370.

Veenman L, Gavish M. The peripheral-type benzodiazepine receptor and the cardiovascular system. Implications for drug development Pharmacol Ther. 2006; 110:503–524.

Verma A, Nye JS, Snyder SH. Porphyrins are endogenous ligands for the mitochondrial (peripheral-type) benzodiazepine receptor. Proc Natl Acad Sci U S A. 1987; 84:2256–2260. [PubMed: 3031675]

Verma A, Snyder SH. Peripheral type benzodiazepine receptors. Annu Rev Pharmacol Toxicol. 1989; 29:307–322. [PubMed: 2543271]

Vlodavsky E, Soustiel JF. Immunohistochemical expression of peripheral benzodiazepine receptors in human astrocytomas and its correlation with grade of malignancy, proliferation, apoptosis and survival. J Neurooncol. 2007; 81:1–7. [PubMed: 16868661]

Wade FM, Wakade C, Mahesh VB, Brann DW. Differential Expression of the Peripheral Benzodiazepine Receptor and Gremlin During Adipogenesis. Obesity. 2005; 13:818–822.

Wang Y, Pan Y, Price A, Martin LJ. Generation and characterization of transgenic mice expressing mitochondrial targeted red fluorescent protein selectively in neurons: modeling mitochondriopathy in excitotoxicity and amyotrophic lateral sclerosis. Mol Neurodegener. 2011; 6:75. [PubMed: 22047141]

Wendler G, Lindemann P, Lacapère JJ, Papadopoulos V. Protoporphyrin IX binding and transport by recombinant mouse PBR. Biochem Biophys Res Commun. 2003; 311:847–852. [PubMed: 14623258]

Woods MJ, Zisterer DM, Williams DC. Two cellular and subcellular locations for the peripheral-type benzodiazepine receptor in rat liver. Biochem Pharmacol. 1996; 51:1283–1292. [PubMed: 8787543]

Yaffe D, Saxel ORA. Serial passaging and differentiation of myogenic cells isolated from dystrophic mouse muscle. Nature. 1977; 270:725–727. [PubMed: 563524]

Yamamura HI, Vickroy TW, Gehlert DR, Wamsley JK, Roeske WR. Autoradiographic localization of muscarinic agonist binding sites in the rat central nervous system with (+)-cis-[$^{3}$H]methyldioxolane. Brain Res. 1985; 325:340–344. [PubMed: 3838491]

Zarbin MA, Anholt RR. Benzodiazepine receptors in the eye. Invest Ophthalmol Vis Sci. 1991; 32:2579–2587. [PubMed: 1651298]

Zhang K, Desurmont T, Goujon JM, Favreau F, Cau J, Deretz S, Mauco G, Carretier M, Papadopoulos V, Hauet T. Modulation of peripheral-type benzodiazepine receptor during ischemia reperfusion injury in a pig kidney model: a new partner of leukemia inhibitory factor in tubular regeneration. J Am Coll Surg. 2006; 203:353–364. [PubMed: 16931308]

Zisterer DM, Williams DC. Peripheral-type benzodiazepine receptors. Gen Pharmacol. 1997; 29:305–314. [PubMed: 9378234]

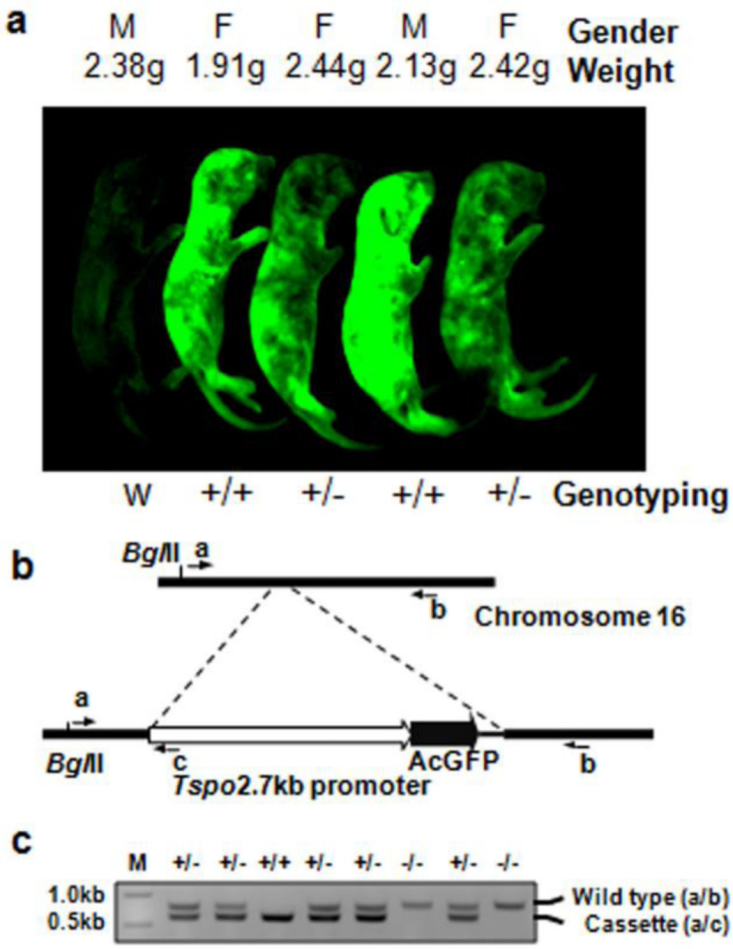


**Fig. 1.**

Transgenic mice synthesizing AcGFP driven by a 2.7-kb region of the *Tspo* promoter and genotyping strategy. **A** Scanning image of AcGFP in green, glowing 6-day-old mouse pups from two heterozygous parents viewed by fluorescence imaging as described under Materials and Methods. **B** Genomic mapping of the *Tspo* promoter-AcGFP transgenic cassette on chromosome 16. The primers used for genotyping are indicated: primers a/b generate a PCR product that indicates that the mouse lacks the transgene and primers a/c generate a PCR product that indicates that the mouse possesses the transgene. **C** Genotyping of transgenic mice using PCR with the three primers as indicated in **B**. One litter of mice generated by heterozygous parents was genotyped as shown here. M, 1kb DNA ladder; +, positive allele with the insertion of *Tspo*-AcGFP cassette; −, wild-type allele

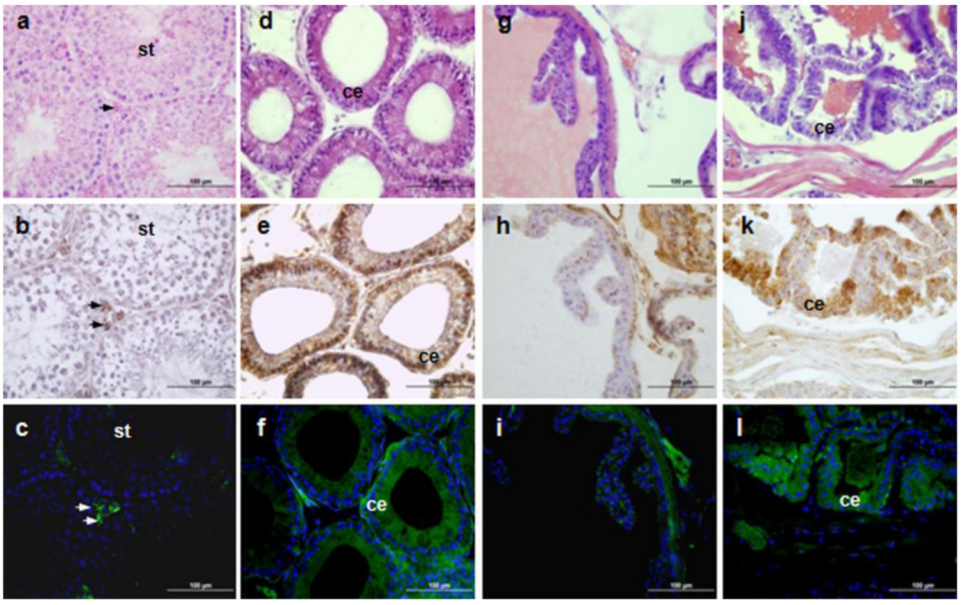


**Fig. 2.**

TSPO immunohistochemical staining and *Tspo*-AcGFP formation in the male reproductive tract. The testis (**A**, **B, C**; arrows indicate interstitial Leydig cells; st, seminiferous tubules), head of epididymis (**D**, **E, F**; ce, columnar epithelium), seminal vesicle (**G**, **H**, **I**), and prostate (**J**, **K**, **L**; ce, columnar epithelium) were examined using H&E staining (**A**, **D**, **G**, **J**), TSPO immunostaining (**B**, **E**, **H**, **K**), and AcGFP presence detected by fluorescence microscopy (**C**, **F**, **I**, **L**)

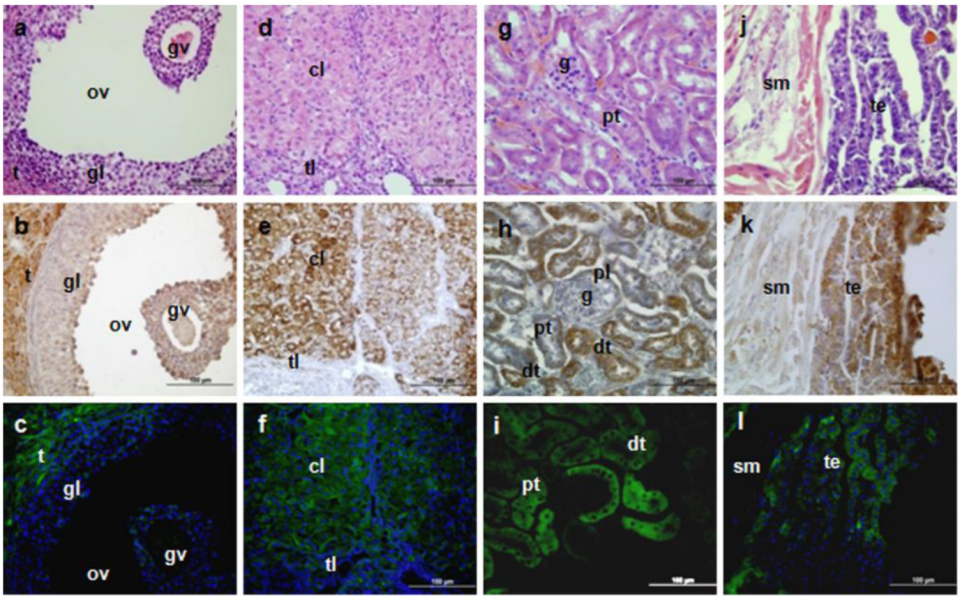


**Fig. 3.**

TSPO immunohistochemical staining and *Tspo*-AcGFP synthesis in the female urogenital system. The ovary (**A–F**; t, theca cells; tl, theca lutein cell; gl, granulosa lutein cells; gv, germinal vesicle; ov, ovarian follicles; cl, corpus luteum), kidney (**G, H, I**; g, glomerulus; pt, proximal tubules, dt, distal tubules; pl, parietal layer of male's glomerulus), and bladder (**J, K, L**; sm, smooth muscle; te, transitional epithelium) were examined using H&E staining (**A**, **D**, **G**, **J**), TSPO immunostaining (**B**, **E**, **H**, **K**), and AcGFP presence detected by fluorescence microscopy (**C**, **F**, **I**, **L**)

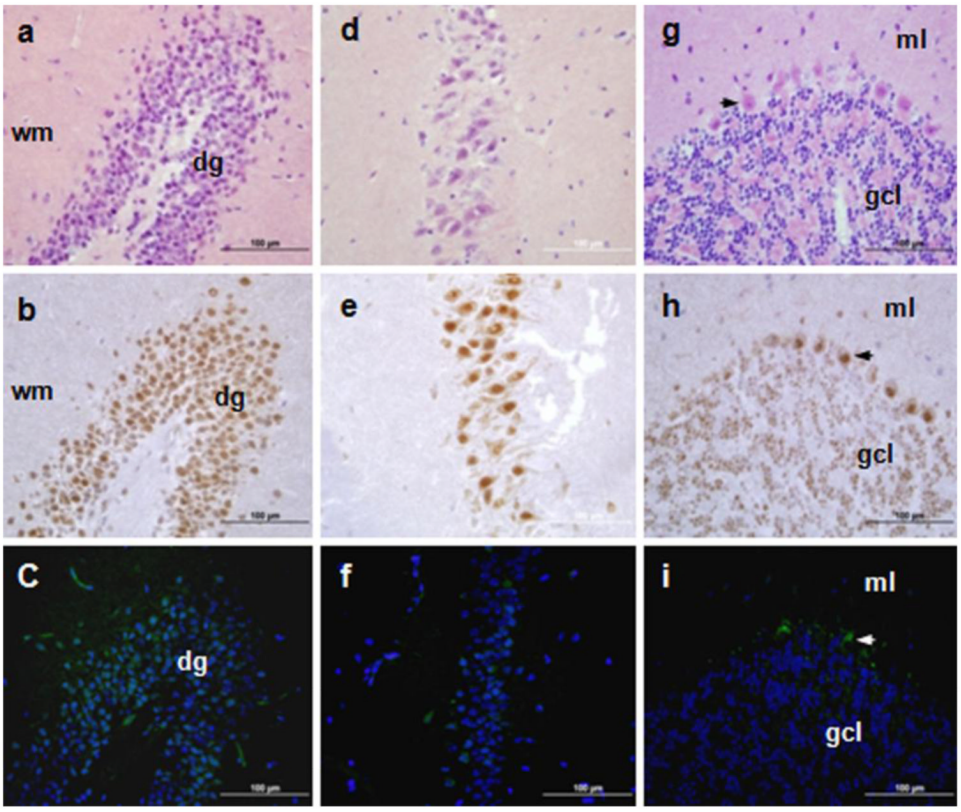


**Fig. 4.**

TSPO immunohistochemical staining and *Tspo*-AcGFP presence in the central nervous system. The hippocampus (**A**, **B, C**; dg, dentate gyrus, wm, white matter), cornu ammonis 3 (CA3) region (**D**, **E**,**F**), and cerebellum (**G**, **H, I**; arrows indicate Purkinje cells; ml, molecular layer; gcl, granule cell layer) were examined using H&E staining (**A**, **D**, **G**), TSPO immunostaining (**B**, **E**,**H**), and AcGFP presence detected by fluorescence microscopy (**C**, **F**, **I**)

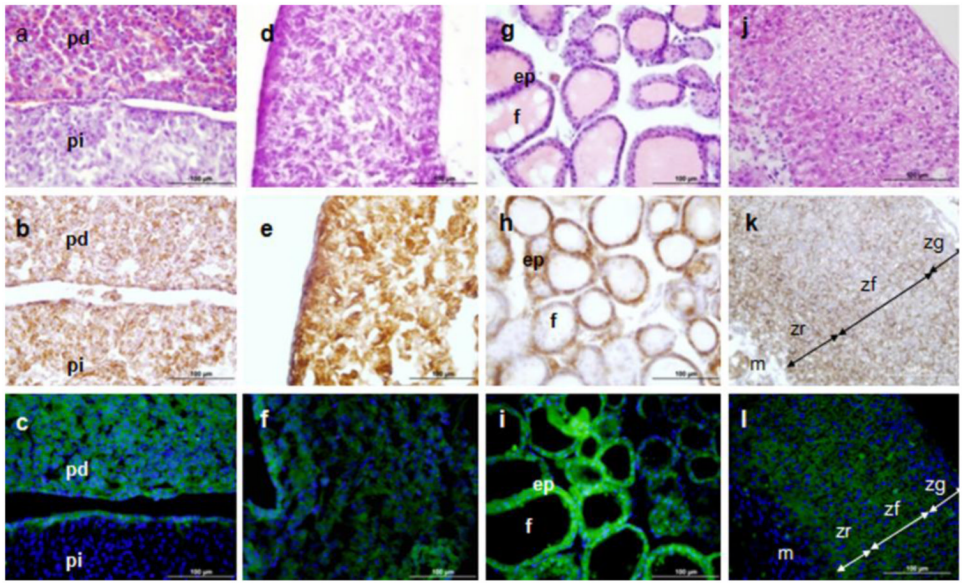


**Fig. 5.**

TSPO immunohistochemical staining and *Tspo*-AcGFP formation in the neuroendocrine and endocrine systems. The pituitary gland (**A**, **B, C**; pd, pars distalis; pi, pars intermedia), pineal gland (**D**, **E, F**), thyroid gland (**G**, **H, I**; ep, epithelium, f, follicles), and adrenal gland (**J**, **K, L**; zg, zona glomerulosa; zf, zona fasciculata; zr, zona reticularis; m, medulla) were examined using H&E staining (**A**, **D**, **G**, **J**), TSPO immunostaining (**B**, **E**, **H**, **K**), and AcGFP presence detected by fluorescence microscopy (**C**, **F**, **I**, **L**)

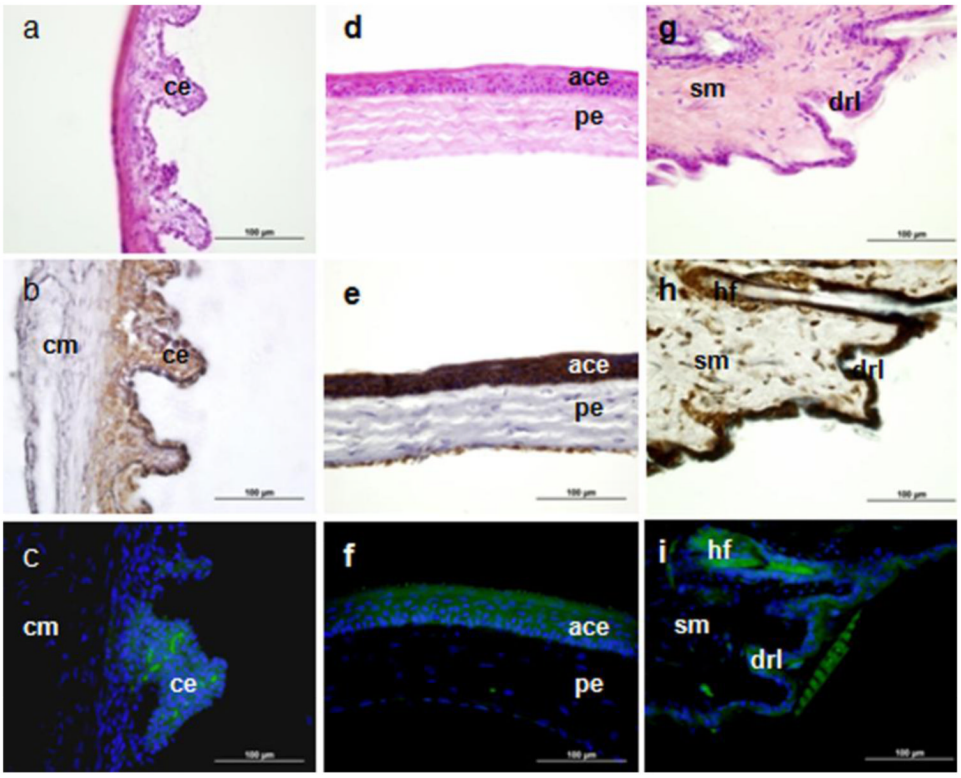


**Fig. 6.**

TSPO immunohistochemical staining and *Tspo*-AcGFP synthesis in the eye and the skin. The ciliary body (**A**, **B, C;** cm, ciliary muscle; ce, ciliary epithelium), cornea (**D**, **E, F;** ace, anterior corneal epithelium; pe, posterior endothelium), and skin (**G**, **H, I;** sm, smooth muscle; hf, hair follicle; drl, dermis reticular layer) were examined using H&E staining (**A**, **D**, **G**), TSPO immunostaining (**B**, **E**,**H**), and AcGFP presence detected by fluorescence microscopy (**C**, **F**,**I**)

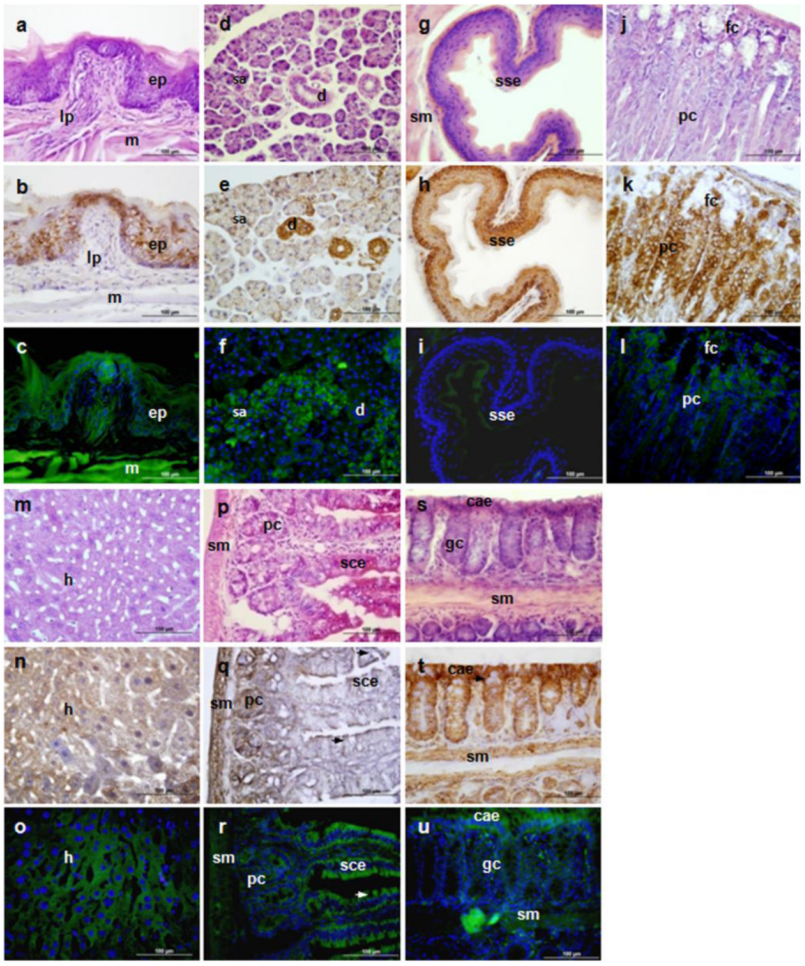


**Fig. 7.**

TSPO immunohistochemical staining and *Tspo*-AcGFP presence in the digestive system. The tongue (**A**, **B, C**; e, epethelium, lp, lamina propria, m, muscle), submandibular glands (**D**, **E, F**; serous gland, male mouse; d, duct, including intercalated portion and striated duct; sa, serous acini), esophagus (**G**, **H, I**; sse, stratified squamous epithelium), stomach (**J**, **K, L**; fc, foveolar cell; pc,parietal cells), liver (**M**, **N, O**; h, hepatocytes), small intestine (**P**, **Q**,**R**; sce, simple columnar epithelium, pc, crypt Paneth cell; sm, submucosa), and colon (**S**, **T, U**; cae, columnar absorptive epithelium, narrows indicate goblet cells; sm, submucosa) were examined using H&E staining (**A**, **D**, **G**, **J**, **M**, **P, S**), TSPO immunostaining (**B**, **E**, **H**, **K**, **N**, **Q**, **T**), and AcGFP presence detected by fluorescence microscopy (**C**, **F**, **I**, **L**, **O**, **R**, **U**)

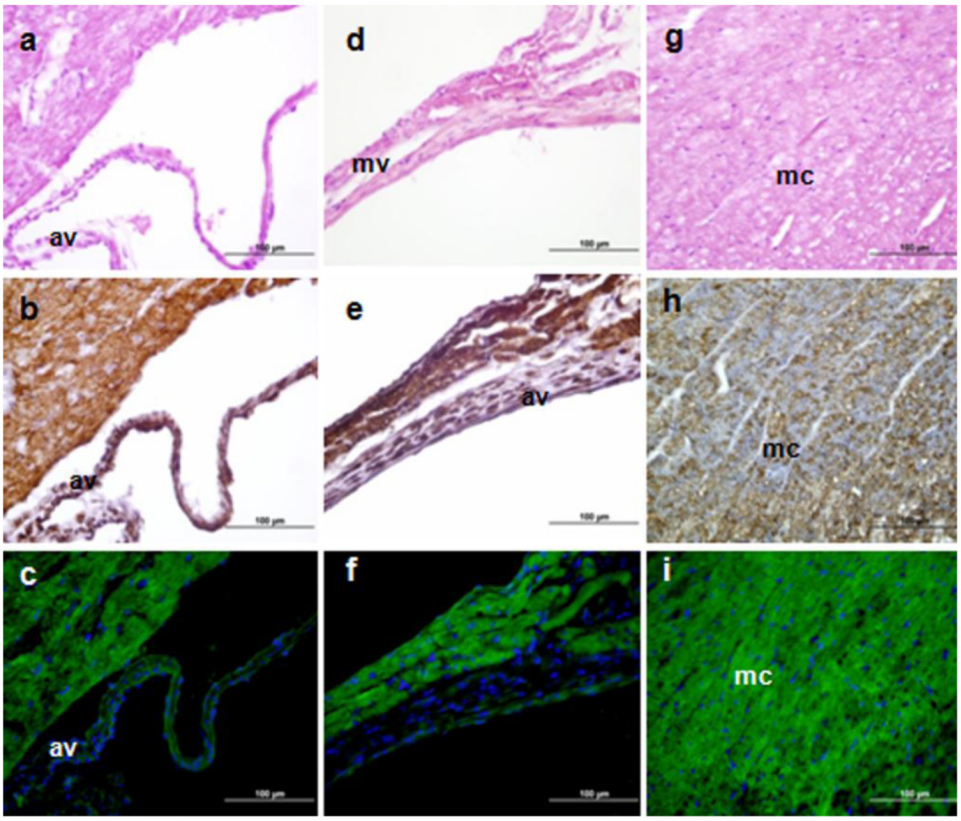


**Fig. 8.**

TSPO immunohistochemical staining and *Tspo*-AcGFP synthesis in the cardiovascular system. Cells were visualized using H&E staining (**A**, **D**, **G**), TSPO immunostaining (**B**, **E**, **H**), and AcGFP presence detected by fluorescence microscopy (**C**, **F**, **I**). av, aortic valve; mv, mitral valve; mc, myocardium

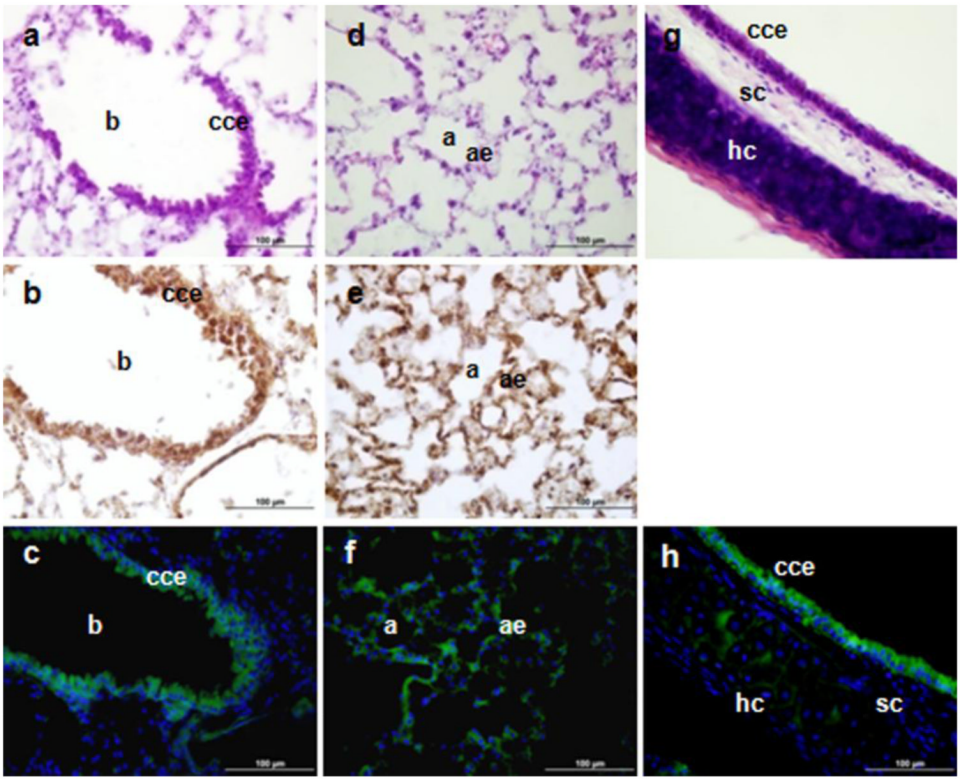


**Fig. 9.**

TSPO immunohistochemical staining and *Tspo*-AcGFP formation in the respiratory system. The lung (**A–F;** b, bronchiole; p, pneumocytes; cce, ciliated columnar epithelium; a, alvolus, ae, type I, II alveolar epithelial cells) and trachea (**G, H;** cce, ciliated columnar epithelium; sc, seromucinous cells; hc, hyaline cartilage) were examined using H&E staining (**A**, **D**, **G**), TSPO immunostaining (**B**, **E**), and AcGFP presence detected by fluorescence microscopy (**C**, **F**, **H**)

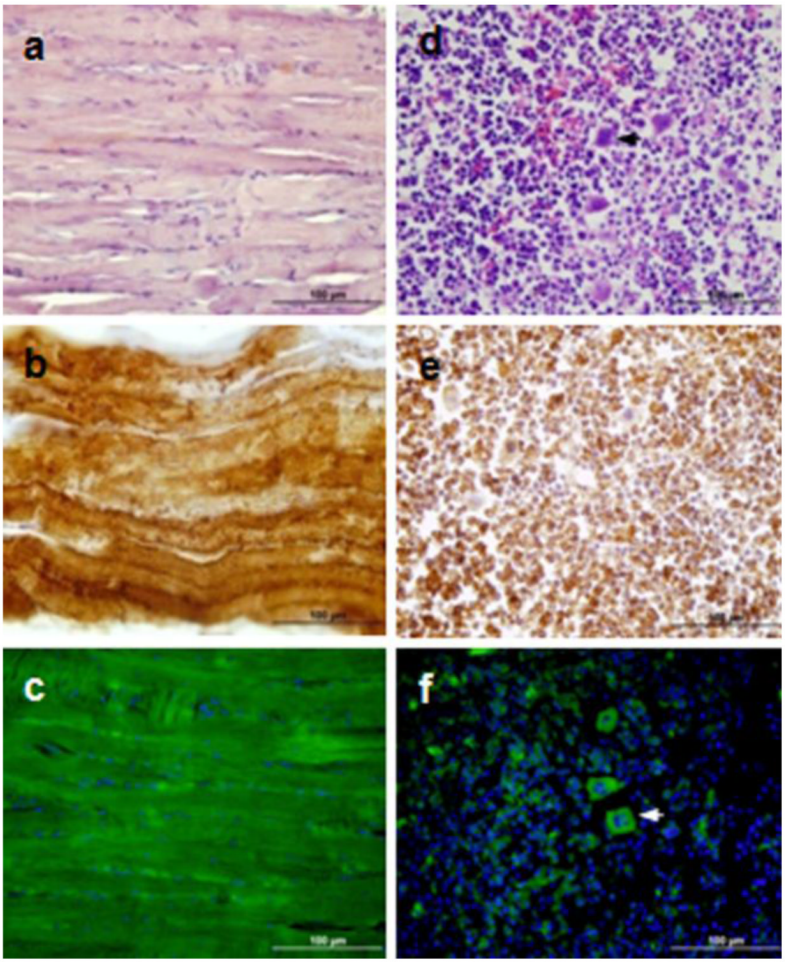


**Fig. 10.**

TSPO immunohistochemical staining and *Tspo*-AcGFP synthesis in skeletal muscle (**A**, **B, C**) and bone marrow (**D**, **E, F**). Arrow indicates megakaryocyte. Cells were examined using H&E staining (**A**, **D**), TSPO immunostaining (**B**, **E**), and AcGFP presence detected by fluorescence microscopy (**C**, **F**).

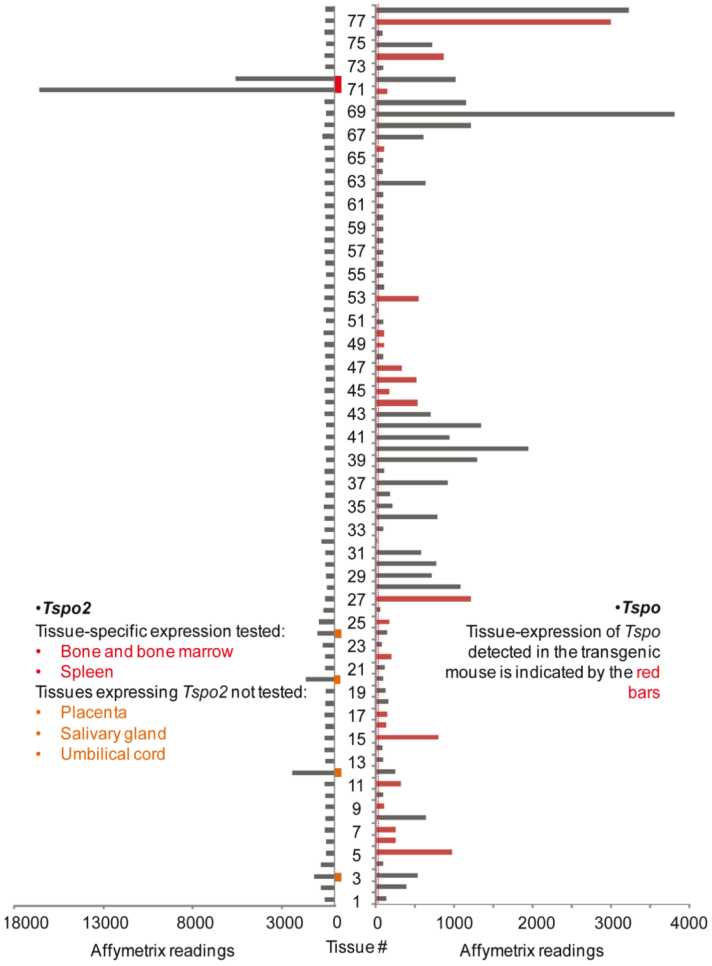


**Fig. 11.**

Expression profiles of *Tspo* and its paralogous gene *Tspo2* in 78 mouse tissues/cell lines. Left panel, the gene atlas of mouse *Tspo2* gene expression in 78 mouse tissues/cell lines. The large-scale analysis of the mouse transcriptome (GNF1M) has been confirmed by our previous report on the *in situ* hybridization of *Tspo2*mRNA in whole-body sections of tissues of all developmental stages (Fan et al. 2009). Right panel, the correlation between AcGFP expression driven by the 2.7-kb region of the *Tspo* promoter and the *Tspo* mRNA atlas from 78 tissues/cell lines was shown in the bar graph representing the Affymetrix GNF1M chip readings, among which the red bars indicate tissues in which *Tspo*-AcGFP was also found to be expressed in the current study. The background signal of Affymetrix readings can be judged from that in oocytes and fertilized eggs, indicated with the red-dotted line. The gene atlases of both *Tspo* and *Tspo2* were retrieved from previously described raw data on the mouse protein-coding transcriptome (Su et al. 2004). The mouse tissues/cell lines are indicated as from number 1 to 78: 1, vomeralnasal organ (VNO); 2, uterus; 3, umbilical cord; 4, trigeminal; 5, trachea; 6, tongue epidermis; 7, thyroid; 8, thymus; 9, testis; 10, substantia nigra; 11, stomach; 12, spleen; 13, spinal cord upper; 14, spinal cord lower; 15, snout epidermis; 16, small intestine; 17, skeletal muscle; 18, septum (respiratory epithelium); 19, septal organ; 20, salivary gland; 21, retina; 22, prostate; 23, preoptic; 24, placenta; 25, pituitary; 26, pancreas; 27, ovary; 28, osteoclasts; 29, osteoblasts_day5; 30,osteoblasts_day21; 31, osteoblasts_day14; 32, oocyte; 33, olfactory bulb; 34, NIH 3T3; 35, neuro2a; 36, medial olfactory epithelium (MOE); 37, mast cells; 38, mammary gland lact.; 39, macrophage unstimulated; 40, macrophage_7hr LPS; 41, macrophage_1hr LPS;

42, M-1; 43, lymph node; 44, lung; 45, liver; 46, large intestine; 47, kidney; 48, hypothalamus; 49, hippocampus; 50, heart; 51, frontal cortex; 52, fertilized egg; 53, epidermis; 54, embryonic stem no feeder; 55, embryonic stem feeder layer; 56, embryo day 9.5; 57, embryo day 8.5; 58, embryo day 7.5; 59, embryo day 6.5; 60, embryo day 10.5; 61, dorsal striatum; 62, dorsal root ganglion; 63, digits; 64, cortex; 65, cerebral cortex; 66, cerebellum; 67, CD8.T cell; 68, CD4.Tcell; 69, C2C12; 70, brown fat; 71, bone marrow; 72, bone; 73, blastocysts; 74, bladder; 75, B220.B cell; 76, amygdale; 77, adrenal gland; 78, adipose tissue.